ARMY RESEARCH LABORATORY

# A Combined Experimental and Numerical Technique to Estimate Interfacial Bond Strength in MMC-Encapsulated Ceramic Systems

**by Brandon McWilliams, Robert Carter, Chian-Fong Yen, and David Gray**

**ARL-TR-6376** **March 2013**

## NOTICES

### Disclaimers

The findings in this report are not to be construed as an official Department of the Army position unless so designated by other authorized documents.

Citation of manufacturer's or trade names does not constitute an official endorsement or approval of the use thereof.

Destroy this report when it is no longer needed. Do not return it to the originator.

**Army Research Laboratory**
Aberdeen Proving Ground, MD 21005-5069

**ARL-TR-6376** **March 2013**

# A Combined Experimental and Numerical Technique to Estimate Interfacial Bond Strength in MMC-Encapsulated Ceramic Systems

**Brandon McWilliams**
**Oak Ridge Institute for Science and Education**

**Robert Carter, Chian-Fong Yen, and David Gray**
**Weapons and Materials Research Directorate, ARL**

| REPORT DOCUMENTATION PAGE | Form Approved OMB No. 0704-0188 |
|---|---|



| 1. REPORT DATE *(DD-MM-YYYY)* | 2. REPORT TYPE | 3. DATES COVERED (From - To) |
|---|---|---|
| March 2013 | Final | March 2011–October 2012 |

**4. TITLE AND SUBTITLE**
A Combined Experimental and Numerical Technique to Estimate Interfacial Bond Strength in MMC-Encapsulated Ceramic Systems

**5a. CONTRACT NUMBER**
ORISE 1120-1120-99

**5b. GRANT NUMBER**

**5c. PROGRAM ELEMENT NUMBER**

**6. AUTHOR(S)**
Brandon McWilliams,* Robert Carter, Chian-Fong Yen, and David Gray

**5d. PROJECT NUMBER**
H84

**5e. TASK NUMBER**

**5f. WORK UNIT NUMBER**

**7. PERFORMING ORGANIZATION NAME(S) AND ADDRESS(ES)**
U.S. Army Research Laboratory
ATTN: RDRL-WMM-B
Aberdeen Proving Ground, MD 21005-5069

**8. PERFORMING ORGANIZATION REPORT NUMBER**
ARL-TR-6376

**9. SPONSORING/MONITORING AGENCY NAME(S) AND ADDRESS(ES)**

**10. SPONSOR/MONITOR'S ACRONYM(S)**

**11. SPONSOR/MONITOR'S REPORT NUMBER(S)**

**12. DISTRIBUTION/AVAILABILITY STATEMENT**
Approved for public release; distribution is unlimited.

**13. SUPPLEMENTARY NOTES**
*Oak Ridge Institute for Science and Education, Oak Ridge, TN 37831

**14. ABSTRACT**
Design and simulation of lightweight composite vehicle armors require mechanical characterization and quantification of the interfacial bond strength between metallic and ceramic components. This report presents a combined numerical and experimental technique to estimate the interfacial strength parameters of a ceramic tile encapsulated by a metal matrix composite. Numerical simulations are used to design an experiment that uses a spherical indenter to introduce shear stresses and cause delamination along the interface without fracturing the underlying ceramic. Indentation experiments are conducted, and the area of the delamination zone observed by post-test c-scan is correlated with parametric simulation results to determine the cohesive zone strength and failure parameters of the interface.

**15. SUBJECT TERMS**
metal matrix composites, encapsulated ceramics, cohesive zone modeling, interface strength, indentation testing

| 16. SECURITY CLASSIFICATION OF: | | | 17. LIMITATION OF ABSTRACT | 18. NUMBER OF PAGES | 19a. NAME OF RESPONSIBLE PERSON |
|---|---|---|---|---|---|
| a. REPORT | b. ABSTRACT | c. THIS PAGE | | | Brandon McWilliams |
| Unclassified | Unclassified | Unclassified | UU | 24 | 19b. TELEPHONE NUMBER (*Include area code*) 410-306-2237 |

**Standard Form 298 (Rev. 8/98)**
Prescribed by ANSI Std. Z39.18

## Contents

## List of Figures

## List of Tables

INTENTIONALLY LEFT BLANK.

# 1. Introduction

Encapsulated ceramics offer potential as mass-efficient vehicle armors. Various means for encapsulating the ceramic to promote beneficial pre-stresses are currently being developed at the U.S. Army Research Laboratory. Direct casting of metal alloys and metal matrix composites are among a few of the materials and processes being investigated. With these approaches, the bond between the matrix and the ceramic tile is unknown. This interfacial bonding is critical for single and multihit ballistic performance. Quantifying the strength of the interface is important for accurate ballistic modeling of residual stress state from processing and the subsequent ballistic performance simulations. The strength of the interface/bond that is formed during the infiltration casting process will be dependent on many variables, such as the specific processing conditions, the wettability of the encapsulate material on the ceramic, surface chemical reactions between the metal and ceramic, and the surface conditions of the materials. Nondestructive evaluation of the cast parts is a valuable tool in determining if a well-bonded interface was formed (i.e., if delamination or interfacial gaps are present) but cannot easily quantify the mechanical strength of the bond.

Traditional techniques for measuring interfacial strength, such as shear, push out, and peel tests, are not suitable for this application as they would require sectioning of the part. Machining of the encapsulated ceramic would relieve the substantial residual stresses built up during casting and could lead to failure of the interface or the ceramic itself. Even if no observable physical damage was created by the machining process, it is still likely that the subsequent measured interfacial strength would be significantly altered from the in situ interface strength in which we are interested. As such, it is desirable to use an alternate technique to estimate the bond strength.

In this report, we present a combined numerical and experimental technique to estimate the interfacial strength parameters of a ceramic tile encapsulated by a metal matrix composite (MMC) material. The goal is to correlate the size of a delamination introduced by using a spherical indenter to damage the interface of a single ceramic tile encapsulated by a thin layer of aluminum MMC. The proposed method uses simulation to determine the optimum indenter size to introduce shear stresses at the ceramic-MMC interface without failing the ceramic. After an appropriate size indenter is selected, indentation experiments are conducted and the delamination zone observed by post-test c-scan is compared with iterative simulation results to determine the cohesive zone parameters for the interface. By correlating the experimentally observed interfacial damage with a finite-element model (FEM), it is then possible to quantify the strength and failure properties of the interface.

## 2. Procedure

### 2.1 Test Specimen Configuration

Individual metal matrix composite encapsulated silicon carbide (SiC) tiles were provided by CPS Technologies of Norton, MA. Each module (figure 1) consisted of a symmetric layup of a hexagonal (3 in flat to flat), 0.75-in-thick SiC tile (BAE) with 0.12 in of Nextel DF-19 (3M) fabric on the front and back faces. The Nextel DF19 fabric is a plain weave fabric produced from Nextel-610 10,000 denier $Al_2O_3$ yarns. Additionally a single layer wrap of Nextel DF-19 (0.019 in) fabric was used around the perimeter. Modules were infiltration cast using Al-2%Cu alloy as the matrix material and were nondestructively evaluated for defects and/or damage using ultrasound (c-scan) when they were received and prior to further testing to establish a baseline. Initial c-scan results (figure 2) showed no evidence of defects or damage in the modules.

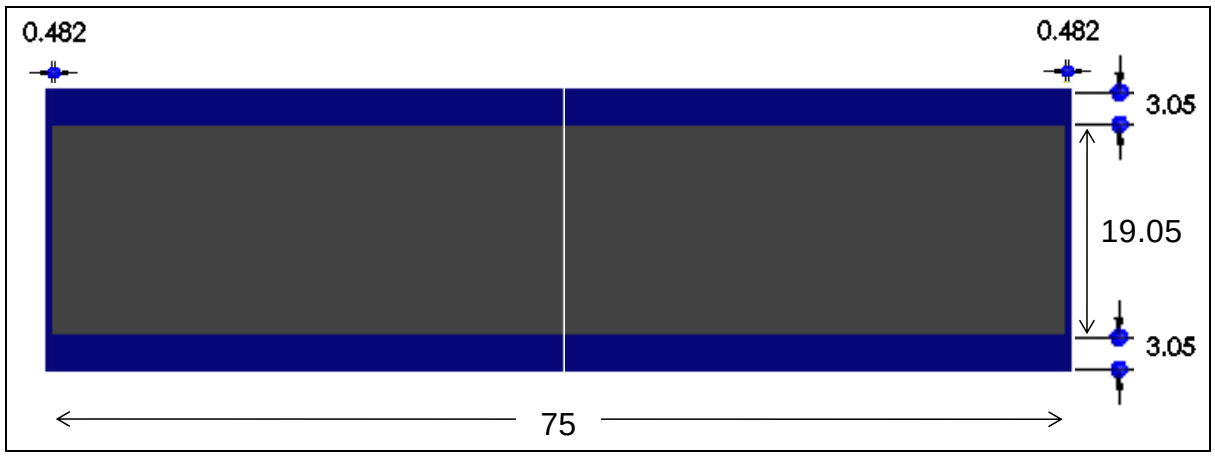


Figure 1. Schematic cross section of individual MMC encapsulated tile. Blue represents Al-Nextel MMC, and grey is SiC tile. All dimensions are in millimeters.

### 2.2 Determination of Optimum Indenter Size

A spherical indenter was chosen for the indentation testing. In order to determine the optimum indenter diameter to maximize interfacial shear stresses and localize failure at the MMC-tile interface without cracking the ceramic tile, a preliminary FEM simulation study was conducted to aid with the design of the experiment. A three-dimensional, one-eighth geometry model of the encapsulated tile was implemented in the commercial FEM code ABAQUS. Simulations were run with three sizes of spherical indenter. Indenter diameters of 0.25, 0.5, and 1 in were considered. The indenter was modeled as a rigid body, and the MMC and SiC were modeled using eight-node, reduced integration brick elements. The interfaces between the MMC

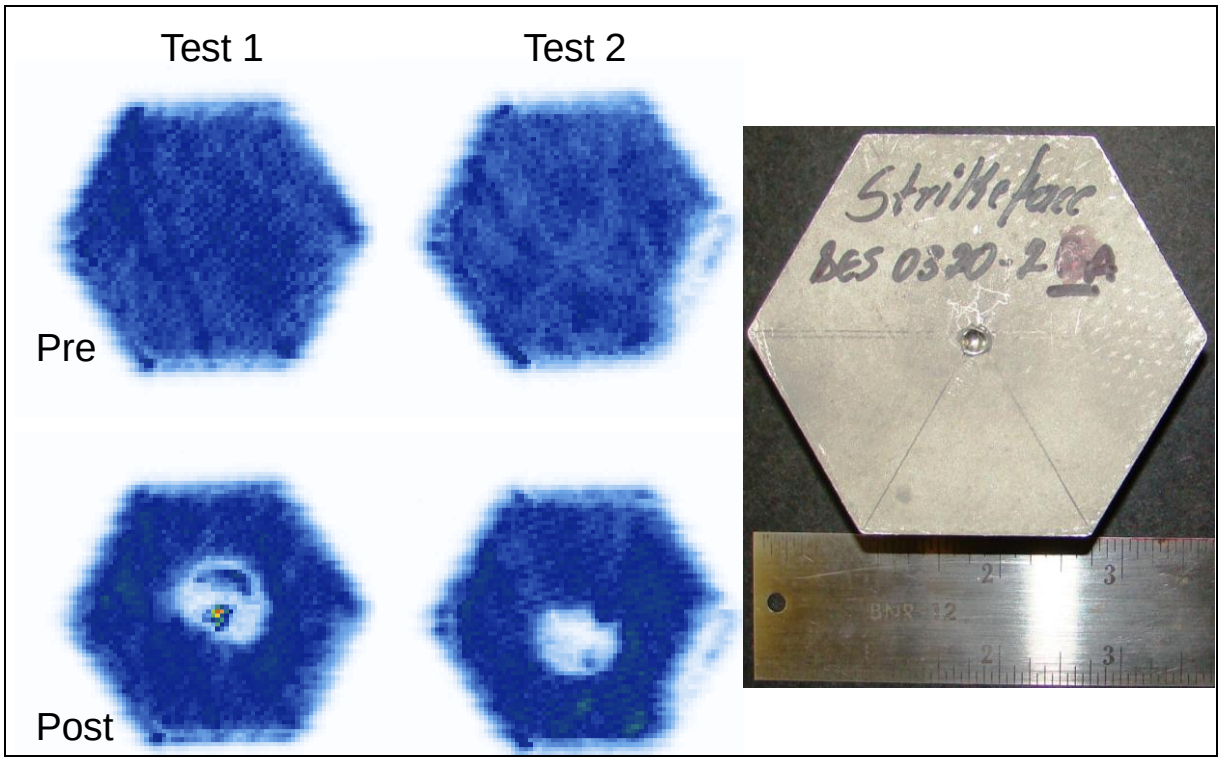


Figure 2. Pre- (top) and post- (bottom) indentation test c-scan (ultrasound) images of MMC encapsulated tiles along with photo of indented module (scale on ruler is in inches). C-scan images are generated from amplitude data from a gate of the rear surface of the module.

and SiC tile were modeled using cohesive zones. The ratio of mesh density of the cohesive zones to the surrounding bodies was ~4:1 using the relations for critical element size presented by Turon et al. (*1*).

The SiC tile was considered isotropic elastic, with density, Young's modulus, coefficient of thermal expansion, and Poisson's ratio, of 3.2 $cm^3$, 449 GPa, $4.0 \times 10^{-6}$ $^oC^{-1}$, and 0.16, respectively. The Johnson-Holmquist-Beissel (JH-B) model (*2*) was used to describe the progressive damage and failure of the tile. The JH-B model considers the effect of hydrostatic pressure (confinement) on the strength of ceramics and was implemented using a user subroutine in ABAQUS.

The sample was cast by CPS Technologies using an infiltration casting process. The tile with a Nextel fabric wrap is placed into a mold. Liquid aluminum is injected into the mold, under pressure, and allowed to solidify. The MMC material used by CPS in the present modules is under development and not yet fully characterized. As such, complete mechanical test data and constitutive models for this material do not presently exist (characterization is an ongoing effort), and it was necessary to estimate properties based on the limited data available in the literature and use micromechanical composite models to fill in the gaps. The MMC material was considered to be elastic-plastic, and progressive damage and failure was not considered. The elastic properties of the Nextel fabric reinforced MMC was considered in-plane orthotropic, with

the *z*-direction being the out-of-plane direction. A micromechanical model based on the Eshelby inclusion theory (*3*) was used to obtain estimates for the orthotropic elastic properties of these composites. The post-yield behavior of the MMC material was assumed to be perfectly plastic (no strain hardening), and the room temperature yield strength for the 35% Nextel MMC was obtained by proportionately scaling the strength of a 60% Nextel DF19 fabric reinforced aluminum MMC found in the literature (*4*). This material had a reported strength of 1500 MPa (in-plane) from which we estimated the yield strength for the 35% material (at room temperature) to be 875 MPa. An anisotropic yield criterion was also implemented to account for the lower strength in the out-of-plane matrix dominated direction. Here the out-of-plane yield was 70% of the in-plane yield strength. A summary of the mechanical properties for 35% (volume) Nextel fabric is given in table 1.

Table 1. Properties for Al-Nextel MMC used in simulations.

| **Matrix** | Al-2%Cu |
|---|---|
| **Reinforcement** | Nextel DF19 woven fabric |
| **Volume Fraction Reinforcement** | 35 |
| **Density (g/cm$^3$)** | 3.3 |
| | |
| **$E_{11}$ (GPa)** | 146 |
| **$E_{22}$ (GPa)** | 146 |
| **$E_{33}$ (GPa)** | 100 |
| **$\nu_{12}$** | 0.19 |
| **$\nu_{13}$** | 0.26 |
| **$\nu_{33}$** | 0.26 |
| **$G_{12}$ (GPa)** | 41.1 |
| **$G_{13}$ (GPa)** | 41.1 |
| **$G_{23}$ (GPa)** | 41.1 |
| | |
| **$\alpha_1$(1 × 10$^{-6}$ °C$^{-1}$)** | 9.6 |
| **$\alpha_2$(1 × 10$^{-6}$ °C$^{-1}$)** | 9.6 |
| **$\alpha_3$(1 × 10$^{-6}$ °C$^{-1}$)** | 16.0 |
| | |
| **$\sigma_y$ (MPa, 20 °C)** | 875 |
| **$\sigma_y$ (MPa, 300 °C)** | 670 |

The constitutive behavior of the cohesive interface zones was modeled using a traction-separation law. Progressive damage and failure of interfaces is generally described by a damage initiation criteria and the energy required for the damage to progress for each mode of fracture (i.e., normal and shear). The cohesive parameters in our test are unknown and will be determined by fitting the experimental data to the simulation predictions. Since our indentation test introduces mixed mode fracture and it is not possible to de-couple the normal and shear modes, damage initiation was specified via a maximum stress criterion ($\sigma_{max}$) and was the same

value for normal and shear modes of failure. The interface was considered brittle, with no further energy ($G_c$) required to fail the cohesive elements. A schematic of the constitutive response of the cohesive elements is shown in figure 3. Once failed, elements are deleted from the mesh, and frictionless contact between the MMC and tile takes over (if applicable).

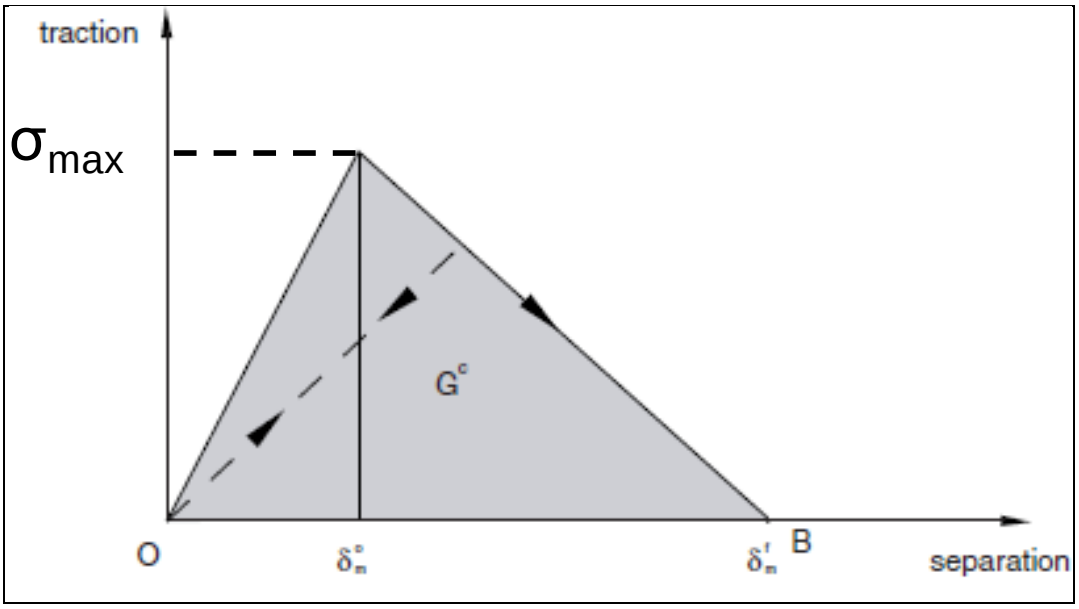


Figure 3. Schematic of the constitutive response of the cohesive elements used in the indentation simulations. Damage initiates at $\sigma_{max}$ and progresses by linear stiffness degradation until complete failure is reached, which is determined by energy required to completely fail the interface (area under the curve, $G_c$).

As there was no a priori way to know the quality of the MMC-tile bond strength, several values of $\sigma_{max}$ were used for each diameter indenter to evaluate the sensitivity of the model to the interface strength. This allowed the determination of the optimum indenter size that would be appropriate over a range of interfacial strengths, from very weak (poor bonding) to very strong (good bonding). The values considered for the maximum stress criteria were 50, 100, and 200 MPa. Figure 4 shows the force displacement curves for the 100-MPa case.

The results of this study show that for all three of the indenter sizes considered, a weak interface ($\sigma_{max}$=50 MPa) results in only interfacial failure (no tile damage) up to large displacements (figure 5). As the strength of the interface increases, SiC tile damage occurs for all diameter indenters (figures 6 and 7); however, the extent of the damage increases as the diameter of the indenter increases. Additionally, the force required for indentation (figure 4) and the rate of interface failure propagation increases with indenter diameter. Thus, the 0.25-in indenter was chosen for the experiments because it is the size most likely to generate stable interface failure, without significant tile damage.

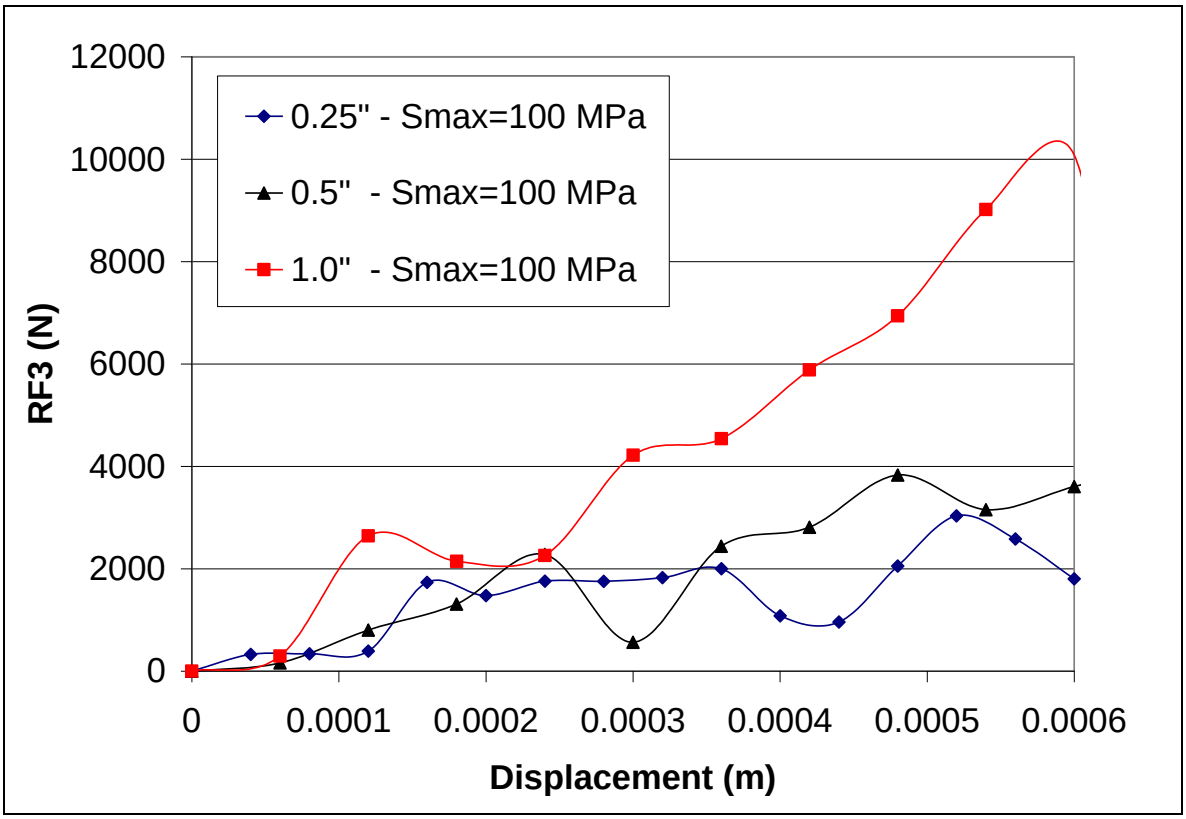


Figure 4. Simulated force displacement curves (reaction force of indenter) for three different diameter indenters with cohesive interface strength of 100 MPa.

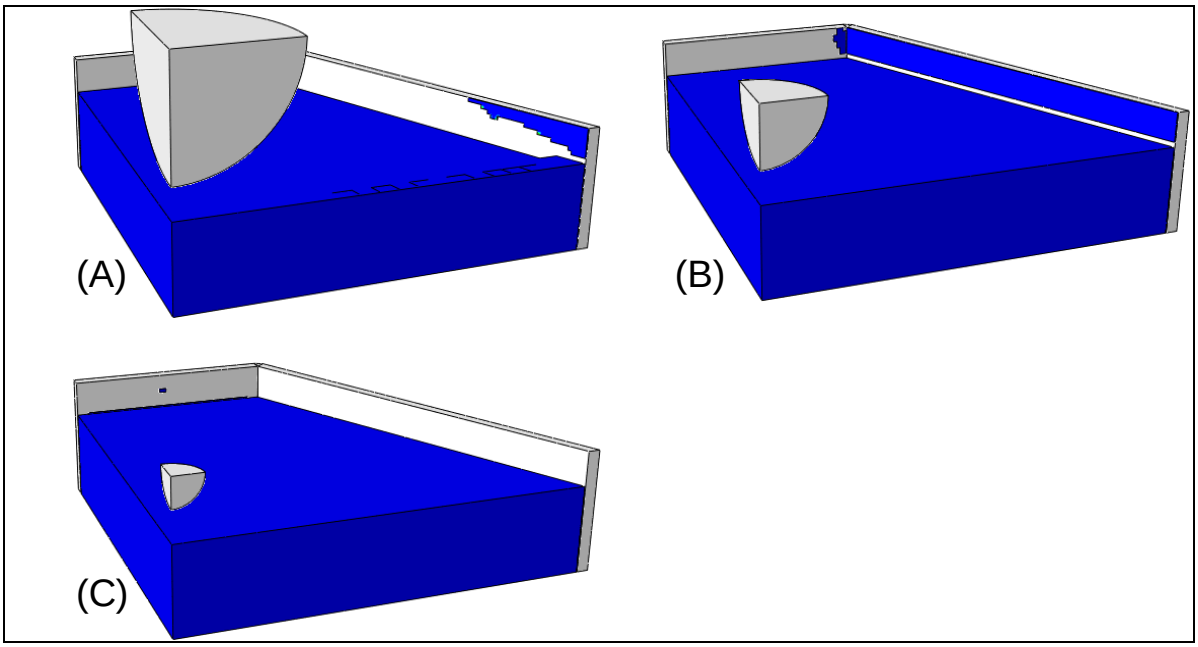


Figure 5. Indentation simulation (one-eighth model) results showing complete interface failure (top MMC layer has been removed for visualization of the interface) for (A) 1-, (B) 0.5-, and (C) 0.25-in-diameter indenters with cohesive strength ($\sigma_{max}$) of 50 MPa at an indenter displacement of 0.4 mm.

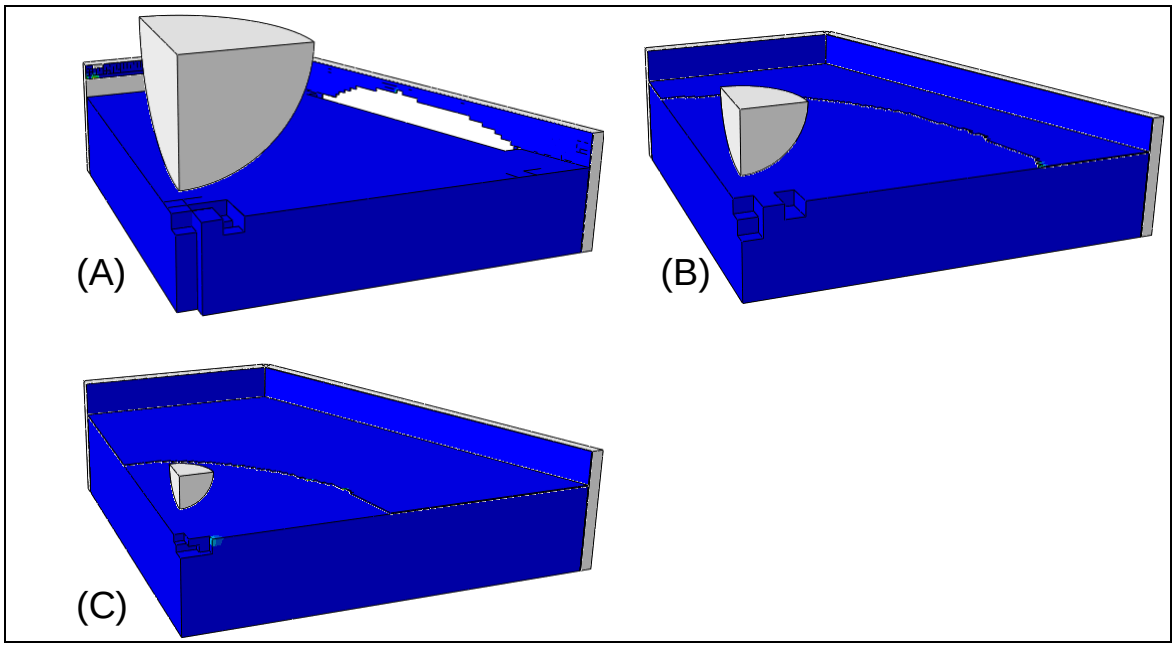


Figure 6. Indentation simulation (one-eighth model) results showing interface failure (top MMC layer has been removed for visualization of the interface) for (A) 1-, (B) 0.5-, and (C) 0.25-in-diameter indenters with cohesive strength ($\sigma_{max}$) of 100 MPa at an indenter displacement of 0.4 mm.

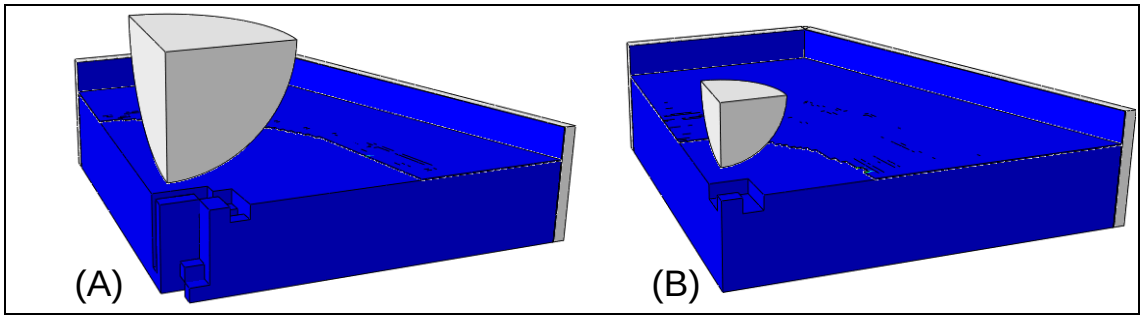


Figure 7. Indentation simulation (one-eighth model) results showing interface failure (top MMC layer has been removed for visualization of the interface) for (A) 1- and (B) 0.5-in-diameter indenters with cohesive strength ($\sigma_{max}$) of 200 MPa at an indenter displacement of 0.4 mm.

### 2.3 Indentation Experiments

Based on the results of the preliminary simulations, a 0.25-in spherical steel indenter was used for the indentation experiments. An Instron load frame was used to indent the center of the encapsulated tile surface at a rate of 0.05 m/s. The test was stopped when the load reached 25 kN, which corresponded to an approximate displacement of 1.5 mm. The test was performed on two modules. The modules were c-scanned post-test to determine the extent and nature of any internal damage.

# 3. Results and Discussion

## 3.1 Determination of Cohesive Zone Parameters

The post-indentation c-scan images (figure 2) show a circular damage zone extending radially outward from the indentation location. Average diameter of this zone was measured by comparing it to the known flat-to-flat distance of the tile. It was found that the average diameters of the damage zone were 24.1 and 21.3 mm for the two tests conducted (average of 22.7 mm). The force displacement curves for these tests are shown in figure 8.

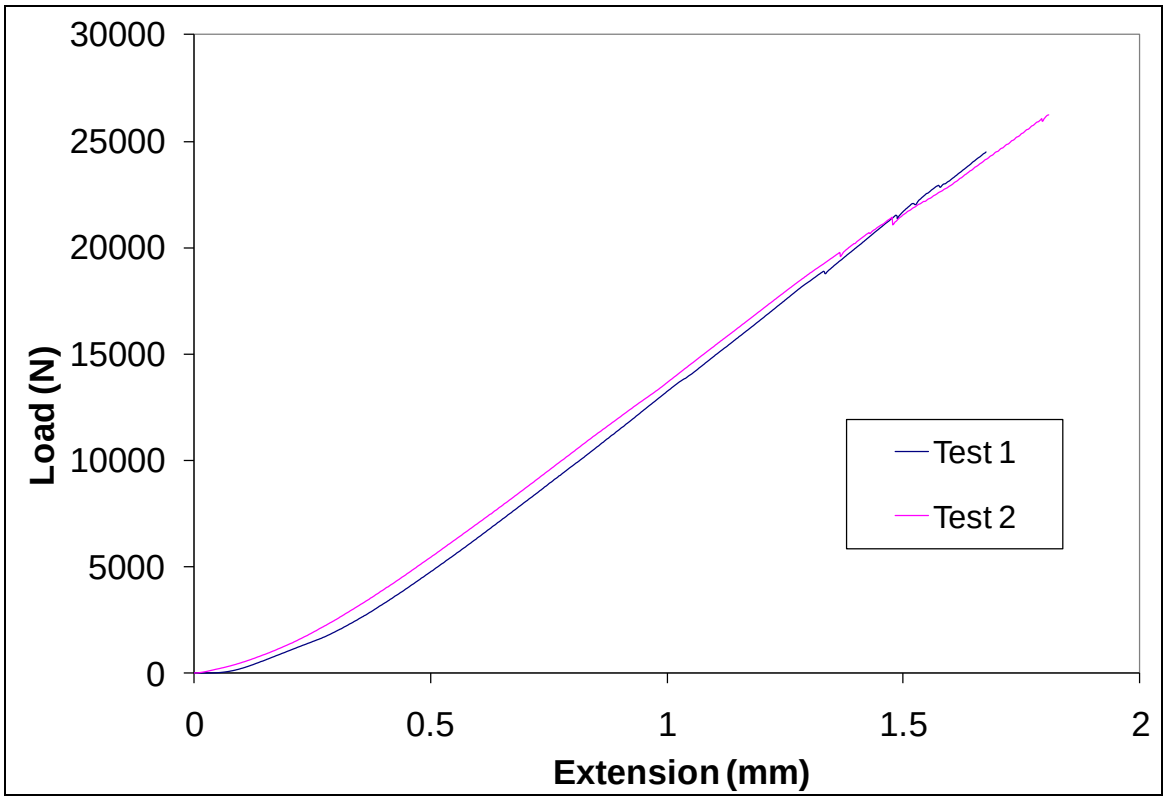


Figure 8. Experimental force displacement curves for 0.25-in indentation tests on two MMC encapsulated ceramic tiles.

The indentation simulations were re-run to find cohesive zone strength and failure parameters that matched the damage pattern observed in the experiments at a displacement of 1.5 mm. Since the interface in the preliminary simulations completely failed at a much lower displacement (~0.5 mm) than in the experiments, it was apparent that the interface strength was higher than the maximum 100-MPa value used for the 0.25-in indenter simulations. To obtain more accurate cohesive parameters, the plastic properties of the Nextel MMC were updated to include multiaxial constitutive behavior for these simulations. Specifically, the plastic behavior of the MMC was modeled to account for the tension-compression yield asymmetry generally

demonstrated by these materials. In this case, the in-plane yield strength of the Nextel fabric MMC was 482 MPa in tension and 325 MPa in compression, which was obtained from testing conducted at the University of Texas at Austin (5). All other material properties and model characteristics were the same as previously discussed.

The compressive yield strength of the MMC (325 MPa) was chosen as a first estimate of the cohesive strength parameter. This resulted in a damage zone diameter of 54.3 mm (figure 9), which is a factor of 2.4 higher than the experimental observation. Increasing the interface strength to 400 MPa resulted in no interfacial failure (figure 9). The strength of the interface was then decreased to 385 MPa, which resulted in a damage zone diameter of 42.3 mm (figure 9) or 1.85× that of the experiment. Based on these results, it was clear that a single cohesive strength parameter was not sufficient to describe the constitutive behavior of the MMC-SiC interface and it would be necessary to determine $G_c$, the fracture energy required for damage progression.

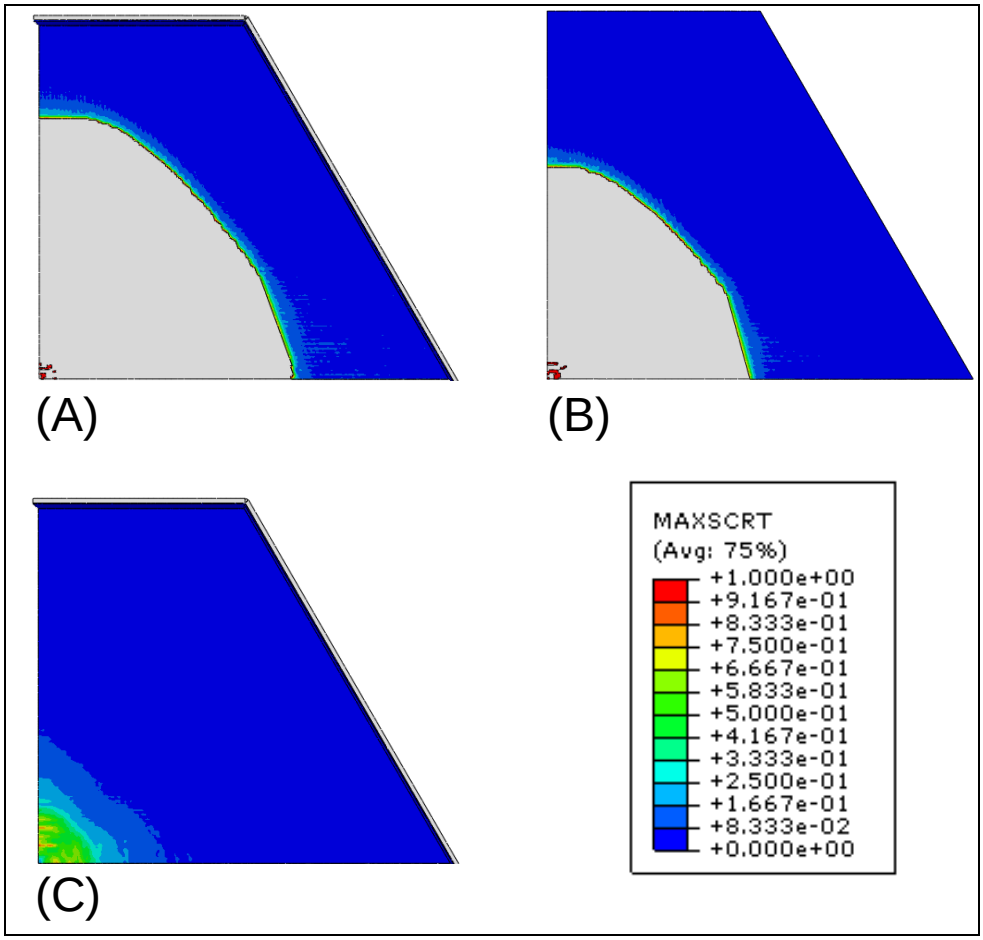


Figure 9. Top view (top MMC layer has been removed for visualization of the interface) of indentation simulation (one-fourth shown) results using a cohesive strength ($\sigma_{max}$) of (A) 325-, (B) 385-, and (C) 400-MPa with zero fracture energy (brittle failure). Contours represent damage initiation criteria (grey regions are failed). Damage initiates when a value of 1.0 is reached.

Based on a single indentation test (mixed mode interface fracture) it is not possible to determine a unique $\sigma_{max}$-$G_c$ combination to describe the interface strength. Rather, it is possible to determine the $G_c$, which gives a good correlation with the experiment for a given $\sigma_{max}$. A value of 300 MPa was assumed for $\sigma_{max}$. Simulations were then carried out, with fracture energies ($G_c$) ranging from 100 to 250 J/m$^2$. By plotting the damage diameter vs. fracture energy (figure 10), we were able to estimate $G_c$ to be 225 J/m$^2$.

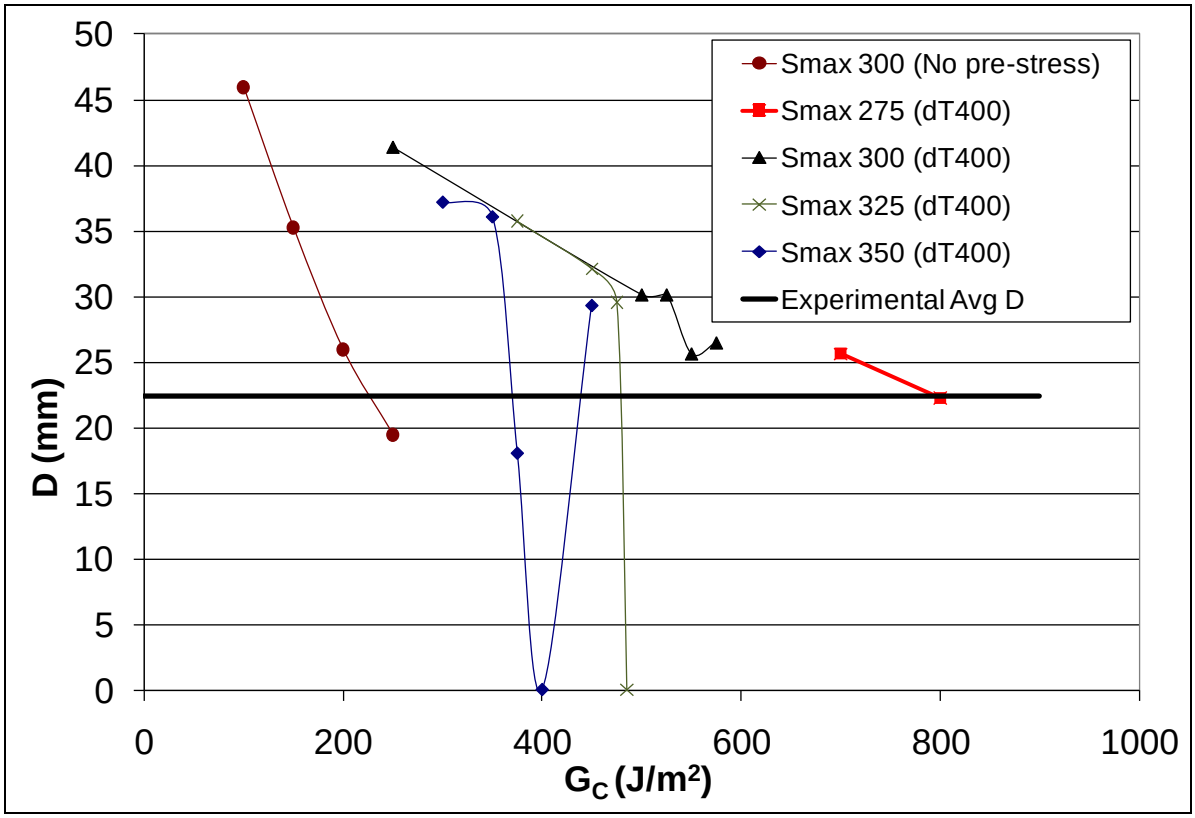


Figure 10. Experimental interface damage diameter vs. simulation parametric study results of interface damage using different cohesive zone parameters.

The calculated values are reasonable with respect to literature data on cohesive modeling of interfaces. For example, Chandra et al. (*6*) found values of 200–400 MPa for $\sigma_{max}$ and values of 640–3000 J/m$^2$ for $G_c$ for titanium-SiC interfaces. Fan et al. (*7*) used values for $G_c$ of 300–500 J/m$^2$ to model fiber composite adhesive joints.

### 3.2 Effect of Residual Stresses

Due to the high temperature of the encapsulation casting process and the large differential in coefficients of thermal expansion (CTE) between the MMC material and the SiC tile, large residual stresses develop in the module as it cools to room temperature. Generally, the CTE of the tile is smaller than the CTE of the MMC material, which results in residual tensile strains in the MMC and compressive residual strains in the tile. Up to this point, these stresses have been

ignored in the determination of the interface parameters. However, it is reasonable to assume that residual stresses and strain relief during loading of the module should have an effect on the damage resulting from the indentation process.

In order to account for thermal residual stresses, a two-part modeling approach is used. First, a thermal-mechanical simulation is run, which applies a temperature change ($\Delta T$) from an assumed stress-free temperature. The residual stress state predicted by this simulation is then imported as the initial stress state in the indentation simulations previously discussed.

The thermo-mechanical model was used to apply a uniform (heat transfer not included) cool down from casting temperature. All interfaces were considered to be perfectly bonded. Time-dependent viscous effects, such as creep, were not considered; a stress-free temperature was assumed rather than cool down from the actual casting temperature (~750 °C). A stress-free temperature of 400 °C was assumed because aluminum does not creep below this temperature. The mechanical properties of the alumina reinforcement fibers of the MMC are independent of temperature up to ~1000 °C. As we are operating well below that threshold, the temperature dependence of the composite material was assumed to follow the aluminum matrix. For the present simulations, the temperature dependence was obtained from tensile data reported for cast A356-T6 alloy (*8*). The temperature dependence of the yield strength of the reference base A356-T6 alloy is shown in table 2.

Table 2. Temperature-dependent mechanical properties of reference cast A356-T6 alloy (*8*).

| **Temperature** | | **Yield Strength ($\sigma_y$)** | |
|---|---|---|---|
| **°C** | **°F** | **MPa** | **ksi** |
| 24 | 75 | 165 | 24 |
| 100 | 212 | 165 | 24 |
| 150 | 300 | 138 | 20 |
| 205 | 400 | 58 | 8.5 |
| 260 | 500 | 35 | 5 |
| 315 | 600 | 21 | 3 |

The residual stress contours from the thermal-mechanical simulation are shown in figure 11. Although the average hydrostatic pressure in the tile is compressive, there are regions in the tile that are in a tensile stress state due to the geometry of the module.

The indentation simulation was then repeated with the new initial stress state. The values of $\sigma_{max}$ and $G_c$, 300 MPa and 250 J/m$^2$, respectively, and determined from the indentation simulations without initial stresses, were used for the cohesive interface properties. This resulted in an interface damage zone with a diameter of 41.4 mm, which is 2.1 times larger than the result of the simulation with the same interface properties but with no initial stresses. This result indicates that residual stresses in encapsulated ceramic modules play a large role in determining interface

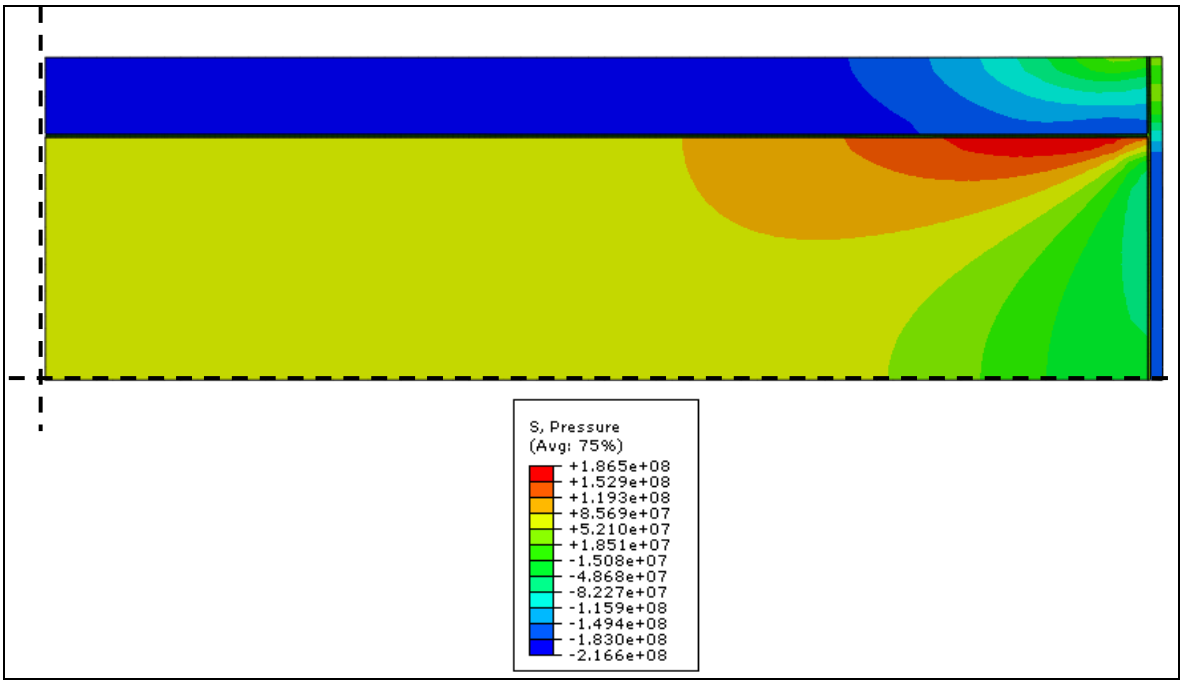


Figure 11. Hydrostatic pressure contours for thermal-mechanical FEM simulation (dashed lines represent symmetry lines in the model) with a ΔT of 400 °C. Convention is that negative values are tensile and positive pressures are compressive.

properties. The $G_c$ parameter was then increased to find the new value which would match the interface damage area to the experimental observation. These results are plotted in figure 10. In contrast to the simulations without initial stresses, the damage zone in the pre-stressed simulations using a $\sigma_{max}$ value of 300 MPa did not decrease in size in a stable manner as the $G_c$ parameter increased, i.e., there were oscillations in the amount of damage vs. fracture energy. A parametric study was conducted to generate damage vs. $G_c$ curves for different values of $\sigma_{max}$ to determine if a $\sigma_{max}$ value could be found which would generate stable interface damage vs. fracture energy response. Increasing $\sigma_{max}$ appears to increase the instability of the interface failure response. For example, with $\sigma_{max}$ of 350 MPa, a $G_c$ of 450 J/m$^2$ resulted in interface failure with a diameter of 29.3 mm, while a $G_c$ of 400 J/m$^2$ resulted in no failure, and a $G_c$ of 375 J/m$^2$ resulted in a damage diameter of 18 mm. In order to generate a stable response, it was necessary to decrease $\sigma_{max}$ to 275 MPa. This is only an 8% decrease from the $\sigma_{max}$ value found using the simulation without pre-stress but results in a 255% increase in the $G_c$ required (800 J/m$^2$) to match the experimentally observed interfacial damage diameter. Higher values of $\sigma_{max}$ result in more stored energy release when interface failure initiates. When failure initiates, the residual stresses from the thermal processing are also relieved, resulting in a complex change in the internal stress state which, in turn, results in the instabilities observed with certain $\sigma_{max}$ and $G_c$ combinations when simulating indentation with an initial stress state.

## 4. Conclusions

A combined experimental and numerical method was developed to determine the interfacial strength parameters for a cohesive zone model of cast metal matrix encapsulated ceramic tiles. The role of thermal residual stresses was shown to play a significant role in determining the interface strength. Values of $\sigma_{max}$ and $G_c$ were found to be 300 MPa and 225 J/m$^2$, and 275 MPa and 800 J/m$^2$ for the indentation simulations with and without initial residual stresses respectively. Interface cohesive strength and failure parameters determined by this method were not considered exact but provided a reasonable quantitative estimate to be used in ballistic/ impact simulations of MMC encapsulated ceramic armor modules.

## 5. References


1. Turon, A.; Davila, C. G.; Camanho, P. P.; Costa, J. An Engineering Solution for Mesh Size Effects in the Simulation of Delamination Using Cohesive Zone Model. *Eng. Fract. Mech* **2007**, *74*, 1665–1682.

2. Holmquist, T. J.; Johnson, G. R.; Beissel, S. R. Characterization and Evaluation of Silicon Carbide for High Velocity Impact. *J. Applied Physics* **2005**, *97* (9), 093502–12.

3. Eshelby, J. D. The Elastic Field Outside an Ellipsoidal Inclusion. *Proceedings of the Royal Society of London*, 1959; Vol. A252, pp 561–569.

4. Deve, H.; McCullough, C. Continuous-Fiber Reinforced Al Composites: A New Generation. *JOM* **1995**, 33–37.

5. Niemczura, J.; Zhang, H.; Ravi-Chandar, K. Mechanical Characterization of Particle and Fabric Reinforced MMCs. Personal communication, University of Texas at Austin, 31 March 2010.

6. Chandra, N.; Li, H.; Shet, C.; Ghonem, H. Some Issues in the Application of Cohesive Zone Models for Metal-Ceramic Interfaces. *Int. J. Sol. and Struct*. **2002**, *39*, 2827–2855.

7. Fan, C.; Ben Jar, P.-Y.; Roger Cheng, J. J. Cohesive Zone With Continuum Damage Properties for Simulation of Delamination Development in Fibre Composites and Failure of Adhesive Joints. *Eng. Fract. Mech* **2008**, *75*, 3866–3880.

8. Kearney, A. L. Properties of Cast Aluminum Alloys, Properties and Selection: Nonferrous Alloys and Special-Purpose Materials. *ASM Handbook*; ASM International, 1990; Vol. 2, pp 152–177.

NO. OF
COPIES ORGANIZATION

1 (PDF) DEFENSE TECHNICAL INFORMATION CTR
DTIC OCA
8725 JOHN J KINGMAN RD
STE 0944
FORT BELVOIR VA 22060-6218

1 (HC) DIRECTOR
US ARMY RESEARCH LAB
IMAL HRA
2800 POWDER MILL RD
ADELPHI MD 20783-1197

1 (PDF) DIRECTOR
US ARMY RESEARCH LAB
RDRL CIO LL
2800 POWDER MILL RD
ADELPHI MD 20783-1197

1 (PDF) GOVT PRINTG OFC
A MALHOTRA
732 N CAPITOL ST NW
WASHINGTON DC 20401

ABERDEEN PROVING GROUND

1 (PDF) DIR USARL
RDRL WMM B
B MCWILLIAMS

INTENTIONALLY LEFT BLANK.